Mitigation of Continuous and Pulsed Radio Interference with GNSS Antenna Arrays

Andriy Konovaltsev [1], David S. De Lorenzo [2],
Achim Hornbostel [1], Per Enge [2]
[1]*German Aerospace Center (DLR), Oberpfaffenhofen, Germany*
[2]*Stanford University, California, USA*

BIOGRAPHIES

Dr. Andriy Konovaltsev received his engineer diploma and the Ph.D. degree in electrical engineering from Kharkov State Technical University of Radio Electronics, Ukraine in 1993 and 1996, correspondingly. He joined the Institute of Communications and Navigation of DLR in 2001. His research interests are in array processing for satellite navigation systems, signal processing algorithms for navigation receivers including synchronisation, multipath and radio interference mitigation.

Dr. David De Lorenzo is a member of the GPS Laboratory at Stanford University. He received a Master of Science degree in Mechanical Engineering from the University of California, Davis, in 1996 and a Ph.D. degree in Aeronautics and Astronautics from Stanford University in 2007. David has worked previously for Lockheed Martin and for the Intel Corporation.

Dr. Achim Hornbostel joined the German Aerospace Centre (DLR) in 1989 after he had received the diploma in Electrical Engineering from the University of Hannover in the same year. In 1995 he received the PhD in Electrical Engineering from the University of Hannover. In 2000 he became member of staff at the Institute of Communications and Navigation at DLR, where he is leading a working group for receivers and algorithms since 2005. He was involved in several projects for remote sensing, satellite communications and satellite navigation. His main activities are currently in signal propagation and receiver development. He is member of VDE/ITG and ION.

Per Enge is a Professor of Aeronautics and Astronautics in the School of Engineering at Stanford University. He directs the GPS Research Laboratory, which develops satellite navigation systems based on the Global Positioning System (GPS). He has been involved in the development of WAAS and LAAS for the FAA. Per is a Fellow of the ION and the IEEE, and has received the Kepler, Thurlow, and Burka Awards from the Institute of Navigation (ION) for his work.

ABSTRACT

A number of antenna array techniques for radio interference mitigation in GNSS receivers have been intensively studied in the last two decades showing that space-only or space-time adaptive processing allows for significant improvements. These investigations were primarily focused on mitigation of continuous interference signals assumed to be of intentional nature in the “quiet” GPS L1 band. In contrast to the L1 band, new navigation signals of GPS/Galileo L5/E5 frequency band have to share the radio spectrum with several civil and military radar systems. In a single-antenna GNSS receiver, the pulsed interference originated from such radar systems is usually handled by using the pulse blanking or frequency extinction techniques. In an antenna array system, more efficient mitigation of pulsed interference can be obtained by adding the spatial domain to the signal processing. In this case, the GNSS antenna array receiver may be designed in a way that allows for simultaneous mitigation of continuous and pulsed interferers. In the paper the performance of two space-time adaptive processing (STAP) techniques has been investigated in interference scenarios with continuous and pulsed sources by using the simulations of a software multi-antenna receiver. It has been shown that the minimum variance distortionless response (MVDR) processor with a corresponding directional constrain delivers both a good performance in term of code and Doppler receiver tracking errors and minimal distortions of the useful GNSS signal. The second investigated STAP technique was minimum mean square error (MMSE) processor. The effect of the number of the STAP time-taps on the performance of the MVDR and MMSE processors has been shown. The combination of the adaptive array processing with the pulse blanking has been examined showing that the simple-to-implement pulse blanking can noticeably improve the overall performance in pulsed interference scenarios.

INTRODUCTION

Satellite navigation is the world’s premier technology for positioning and timing. Global Satellite Navigation Systems (GNSS) are able to provide typical accuracies of meters in position and nanoseconds in time. These accuracies make the use of GNSS being very attractive

for a large and continuously growing number of diverse applications. This growing dependency on the GNSS technology has raised concerns about the vulnerability of the provided positioning and timing services to radio frequency interference (RFI). This stems from fact that the GNSS signals travelling from MEO satellites are very weak at the output of the receiver antenna and can be easily jammed even with low-power radio transmissions from the user vicinity. The interference is usually of unintentional nature, e.g. due to the spectrum sharing with other radio systems, but might be also produced deliberately. Especially challenging is the problem of radio interference in the field of safety-of-life GNSS applications.

One of the most powerful technologies against radio interference is the multi-element antenna arrays with adaptive beam-forming and null-steering capabilities. The constant evolution of the digital processing hardware opens the door for the implementation of the corresponding techniques at acceptable price.

A number of antenna array techniques for radio interference mitigation in GNSS receivers have been intensively studied in the last two decades showing that space-time adaptive processing allows for significant improvements (see [1]-[4] and references herein). These investigations were primarily focused on mitigation of continuous interference signals assumed to be of intentional nature in the "quiet" GPS L1 band. In contrast to the L1 band, new navigation signals at GPS/Galileo L5/E5 have to share the radio spectrum with other radio systems of the Aeronautical Radionavigation Services (ARNS). The most significant in-band interference in the L5/E5 band is originated from the pulsed Distance Measuring Equipment (DME) and Tactical Air Navigation (TACAN) systems [5]. DME is a civil aviation system; together with its military counterpart TACAN it is used for aircraft navigation by providing the measurement of the slant range between an aircraft and the ground station (transponder). The sites of the DME/TACAN stations are the most densely distributed over the US, Europe and Japan. If a ground GNSS receiver is located at the area with intensive flight traffic, signals from several DME/TACAN stations can be observed at the antenna output of the receiver with power levels lying significantly above the noise floor [6].

In this paper we investigate the performance of two space-time adaptive processing (STAP) techniques in the signals scenarios with both continuous and pulsed (DME/TACAN) types of radio interferences. In this study the number of antenna elements in the adaptive array was adopted to be equal to four like in the demonstrator of a Galileo L1/E5 antenna array receiver that is currently developed by DLR [7]. Because of the fixed number of the array elements, we were interested in the investigation of the effect of the number of time-taps in the STAP structure on the interference mitigation performance. Especially with the relatively narrowband DME/TACAN interfering signals having the most of energy inside the double-side bandwidth of 0.8 MHz, the interest was in determining whether the efficient mitigation may be provided just by increasing the temporal degrees of freedom in STAP.

In a single-antenna GNSS receiver, the DME/TACAN interference is often handled by utilising the temporal pulse blanking that is a method which is simple in implementation but sufficient in many practical cases. Therefore, the combination of the pulse blanking with the space-time adaptive processing is also investigated in this paper.

The reminder of the paper is organised as follows. The next section introduces the signals model and describes the STAP techniques which were used in this study. Afterwards, the details about the computer simulations with the use of a multi-antenna software receiver will be given. Then the obtained simulations results for different interference scenarios with continuous and pulsed interference signals will be presented. Finally, the main results of the reported study will be summarised in the last section.

SPACE-TIME ADAPTIVE PROCESSING TECHNIQUES

The model of a GNSS receiver with space-time adaptive processing is shown in Figure 1. The array consists of M antenna elements and each element is backed by a RF frontend that performs down-conversion, signal conditioning and analogue-to-digital conversion (ADC). Please note that the number of array elements, M, is assumed to be 4 in this study. The digitalised output of each RF frontend is fed into an adaptive finite impulse response (FIR) filter with K time taps. The signals after the FIR filters are summed up in order to obtain the output of the space-time adaptive processor. Further, we assume that an independent STAP structure is used in each digital signal processing channel of the GNSS receiver. The space-time adaptive processor in the receiver channel is then optimised for the reception of a specific navigation satellite. The digital STAP output can be mathematically described as follows:

$$y[n] = \sum_{m=1}^{M}\sum_{k=1}^{K} w_{mk} x_m[n-k+1] = \mathbf{w}^T\mathbf{x} \qquad (1)$$

where w_{mk} denotes the STAP weight at the kth tap of the FIR filter after the mth array element (see also Figure 1), $x_m[n]$ is the nth sample of the mth array element output, and the STAP input and weight $MK \times 1$ vectors, $\mathbf{x}$ and $\mathbf{w}$ correspondingly, are defined as:

$$\begin{aligned}\mathbf{x} &= [x_1[n],\ldots,x_1[n-K+1],\ldots,x_M[n],\ldots,x_M[n-K+1]]^T \\ \mathbf{w} &= [w_{11},\ldots,w_{1K},\ldots,w_{M1},\ldots,w_{MK}]^T\end{aligned} \qquad (2)$$

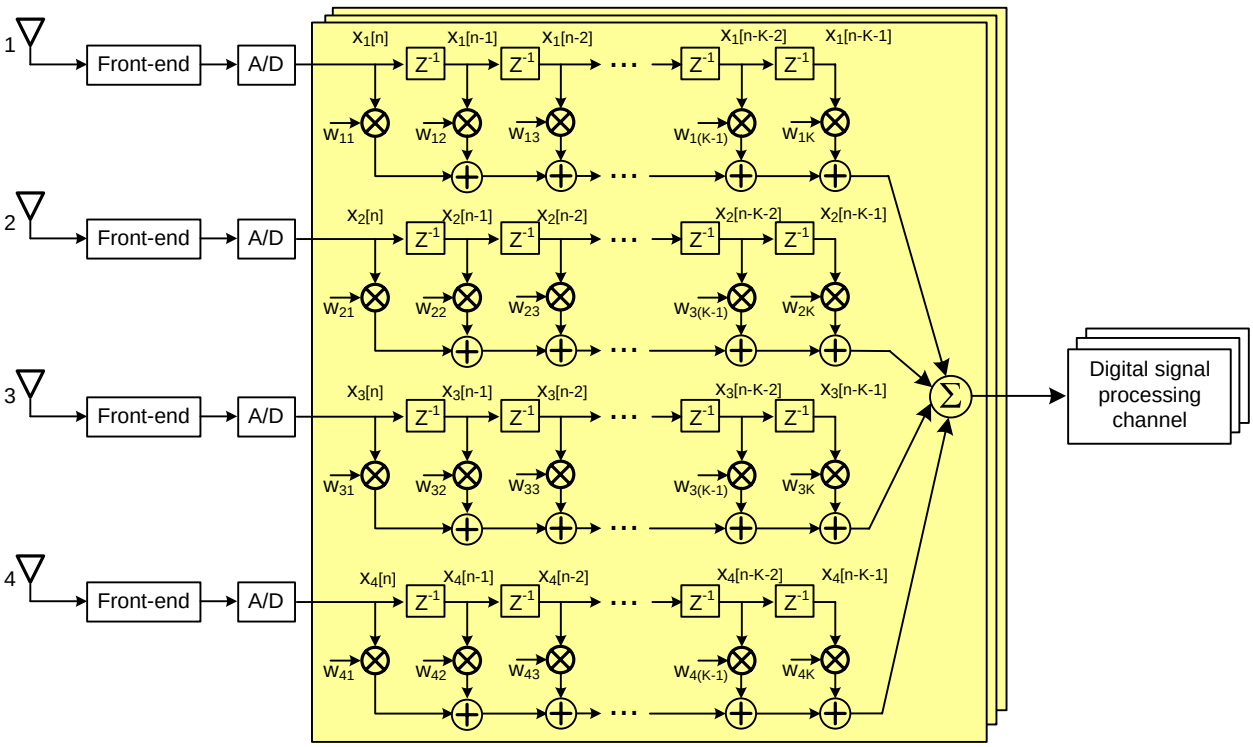

Figure 1: GNSS receiver with space-time array processing

The performance and behaviour of the space-time adaptive processor is determined by the control algorithm used to update the STAP weights (see Figure 2).

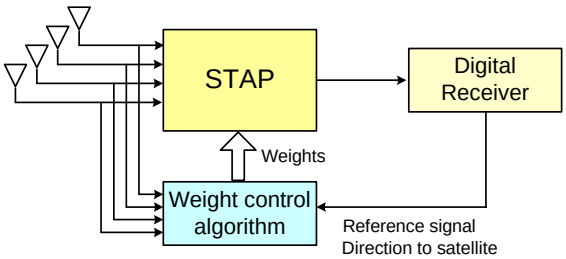

Figure 2: STAP weight control algorithm

Two following weight control algorithms are adopted in this paper:

- minimum mean square error (MMSE) algorithm that adjusts the STAP weights in order to minimise the mean square difference between the desired reference signal s_{ref} and the STAP output [1];
- minimum variance distortionless response (MVDR) technique (often also referred to as Capon beamformer) that minimises the STAP output power while preserving a predefined gain at the desired direction.

The STAP weights with these algorithms are obtained as the solution of the following optimisation problems:

- MMSE algorithm:

$$\mathbf{w}_{opt} = \arg\min_{\mathbf{w}} \mathrm{E}\left\{ \left| s_{ref} - \mathbf{w}^T \mathbf{x} \right|^2 \right\} \tag{3}$$

$$\mathbf{w}_{opt} = \mathbf{R}^{-1}\mathbf{g}_s \tag{4}$$

- MVDR algorithm [8]:

$$\mathbf{w}_{opt} = \arg\min_{\mathbf{w}} \mathbf{w}^H \mathbf{R}\mathbf{w} \quad \text{subject to } \mathbf{w}_i^T \mathbf{a} = 1 \text{ and } \mathbf{w}_j^T \mathbf{a}\Big|_{j\neq i} = 0 \tag{5}$$

$$\mathbf{w}_{opt} = \mathbf{R}^{-1}\mathbf{C}\left(\mathbf{C}^H \mathbf{R}^{-1}\mathbf{C}\right)^{-1}\mathbf{f} \tag{6}$$

$$\mathbf{C} = \begin{bmatrix} \mathbf{a} & \mathbf{0} & \cdots & \mathbf{0} \\ \mathbf{0} & \mathbf{a} & \cdots & \mathbf{0} \\ \mathbf{0} & \mathbf{0} & \ddots & \mathbf{0} \\ \mathbf{0} & \mathbf{0} & \cdots & \mathbf{a} \end{bmatrix}_{MK\times K} \tag{7}$$

$$\mathbf{f} = \begin{bmatrix} f_1 & f_2 & \cdots & f_K \end{bmatrix},\ f_i = 1,\ f_{j\neq i} = 0 \tag{8}$$

where $\mathbf{R} = \mathrm{E}\{\mathbf{x}\mathbf{x}^H\}$ is the STAP covariance matrix; $\mathbf{g}_s = \mathrm{E}\{\mathbf{x}s_{ref}\}$ is the cross-correlation vector between the STAP input and the reference signal; $\mathbf{w}_i = [w_{1i}, w_{2i}, w_{3i}, w_{4i}]^T$ is the weight vector at the i th tap that is the central tap in the STAP FIR filters; $\mathbf{a}$ is a

$M \times 1$ array steering vector in the desired direction and $\mathbf{0}$ is a $M \times 1$ vector with all nulls.

In a practical implementation, the covariance matrix $\mathbf{R}$ and the cross-correlation vector $\mathbf{g}_s$ should be estimated by using observations of the STAP input $\mathbf{x}$. In this study we utilised the block adaptation in the recursive least squares manner defined as follows:

$$\hat{\mathbf{R}}[l+1] = \gamma \hat{\mathbf{R}}[l] + \mathbf{X}[l]\mathbf{X}^H[l] \quad (9)$$

$$\hat{\mathbf{g}}_s[l+1] = \gamma \hat{\mathbf{g}}_s[l] + \mathbf{X}[l]\mathbf{s}_{ref}[l] \quad (10)$$

where γ is a memory factor that defines to which extent the older estimations are accounted for obtaining a new one, γ = 0.9 was adopted further; $\mathbf{X}[l]$ is a $MK \times N$ matrix that collects N STAP inputs over some adaptation time interval; $\mathbf{s}_{ref}[l]$ is a $N \times 1$ vector containing N samples of the reference signal in the adaptation interval. The value of 1 ms was adopted for the block adaptation interval.

SIMULATION SETUP

The simulations described in this paper have been performed in MATLAB environment. The block diagram of the simulation setup is shown in Figure 3. The setup consists of two main blocks: the software signal generator and the GNSS receiver.

The signal generator was used to simulate baseband digital signals at outputs of a 2-by-2 rectangular antenna array. Three generator sub-blocks are used to produce a specific type of signals:

- Galileo E5a signal block generates the ranging codes according to Galileo Open Service SIS ICD [9].
- Block of wideband and narrowband continuous wave (CW) interference generates a specified number of the corresponding interference signals at the carrier frequencies defined by the user.
- DME signals block produces trains of DME/TACAN pulse pairs by using the Gaussian pulse form as described in [5][6]. For simplicity, the amplitude modulation of the TACAN pulses was not simulated. In order to allow a realistic simulation of the collision effect of pulses from multiple DME/TACAN stations, the positions of pulse pairs in the train were modelled as Gaussian random variables with the expected values predicted by the station pulse repetition frequency (PRF).

The geometry of the 2-by-2 array with half wavelength separation between the elements in the rectangular grid is depicted in Figure 4. Since the investigation of antenna effects on the STAP performance was out of scope of the current work, the following simplifying assumptions regarding the antenna array have been made:

- the array elements are isotropic;
- electromagnetic mutual coupling between array elements is negligible;
- the hardware of the antenna channels is perfectly calibrated.

An accurate wideband modelling of the array signals by accounting for the signal propagation time over the array aperture and corresponding time delays between the array elements was used.

A finite impulse response filter with linear phase response and the single-side bandwidth of 12.5 MHz has been used to simulate the RF frontend filter. The generated complex samples of the array signals at 30 MHz rate were stored on a PC hard disk with the 32-bit resolution in the floating point format in order to allow for the simulations of the pulse blanking, adaptive gain control and analogue-to-digital conversion effects in the software receiver.

The space-time adaptive processing was applied prior to the PRN code correlation. The STAP output was fed into the Galileo E5a signal processing block where a conventional PLL/DLL tracking architecture with 1 chip early-late correlator spacing and 20 ms coherent integration time is used. The pilot Q-channel of the Galileo E5a signal was utilised for the tracking. The bandwidths of the tracking loop filters were set to 1 Hz and 7 Hz in DLL and PLL, correspondingly. The following outputs of the tracking block were used to assess the performance of the STAP algorithms: carrier to noise density ratio (C/N_0), code and Doppler tracking errors.

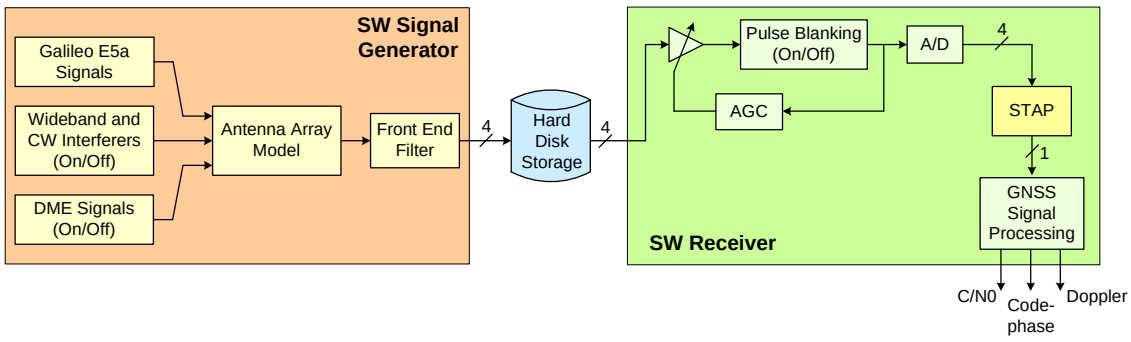

Figure 3: Block diagram of simulation setup

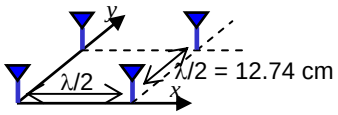

Figure 4: Array model

The parameters of Galileo E5a and interfering signals adopted for the simulations are summarised in Figure 5. The carrier-to-noise density ratio of 42 dB-Hz used with the Galileo E5a signals and interference-to-noise ratios used with continuous and pulsed interfering signal are specified at the output of the frontend filter, i.e. before the analogue-to-digital conversion block.

Unless otherwise indicated, an 8-bit ADC resolution was used in the simulation signal scenarios.

Galileo Satellites

C/N0 = 42 dB-Hz

PRN	Azimuth	Elevation
1	0	40
2	30	30
3	60	40
4	90	50
5	120	20
6	150	60
7	210	70
8	240	20
9	270	30
10	300	80

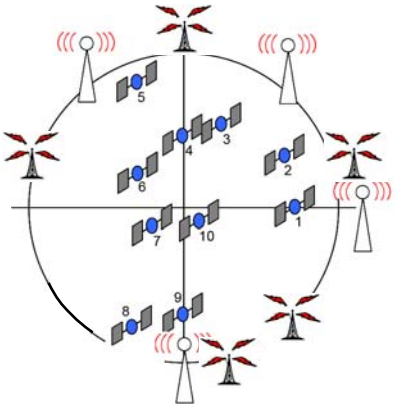

a) Parameters of Galileo E5a signals.
Sky plot with the Galileo satellites and interferers

DME Interferers

DME	Azimuth	Elevation	Freq. Offset	Pulse INR, dB	PRF, Hz
1	15°	5°	-2.45 MHz	20 dB	2700
2	150°	2°	-6.45 MHz	10 dB	2700
3	250°	5°	5.55 MHz	30 dB	3600
4	330°	2°	8.55 MHz	5 dB	2700
5	90°	2°	1.55 MHz	15 dB	3600

b) Parameters of pulsed DME interfering signals

Continuous Interferers

RFI	Azimuth	Elevation	Freq. Offset	Bandwidth
1	0°	5°	0 MHz	CW
2	45°	3°	0 MHz	20 MHz
3	120°	2°	5 MHz	CW
4	270°	10°	0 MHz	20 MHz

c) Parameters of continuous interfering signals

Figure 5: Signal parameters

SIMULATION RESULTS

Interference-free scenario

The results for the interference-free case where only the signals of Galileo E5 satellites with PRNs from 1 to 10 with C/N_0 = 42 dB-Hz (see Figure 5a) were simulated are presented in Figure 6, Figure 7 and Figure 8. As can be seen from Figure 6, from the two tested algorithms the MVDR technique delivers slightly better performance. While with the MVDR algorithm the performance metrics stay unchanged over the number of STAP time taps, the same metrics degrade slightly in the case of MMSE option. For the code root mean square error (RMSE) this occurs mostly because of the error bias increase as shown in Figure 7. The magnitude and phase of the STAP frequency response in the direction of arrival of the satellite with PRN 1 (0° azimuth and 40° elevation) are presented in Figure 8. Very flat responses both in magnitude and phase causing only some minimal distortions of the Galileo E5a signal can be observed with the MVDR algorithm. In the case of MMSE technique, the STAP amplitude response is close by the form to the spectral density of the Galileo E5a BPSK(10) signal; the phase of the STAP response is quite flat in the region of ±10 MHz of the main-lobe of the BPSK(10) spectral density.

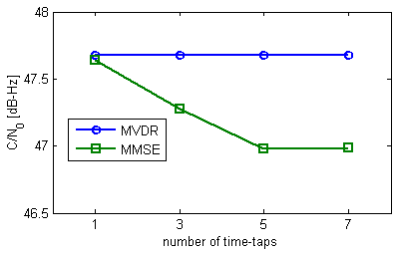

a) C/N_0

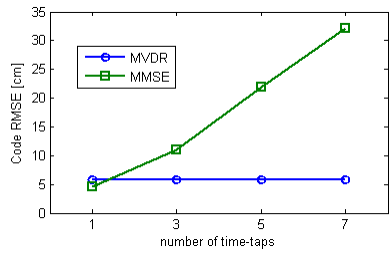

b) code error

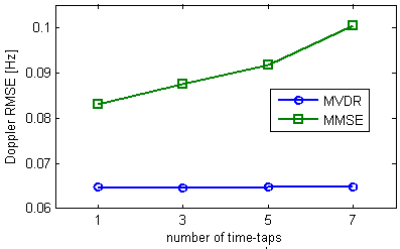

c) Doppler error

Figure 6: Interference-free scenario.
Results are averaged over 4 satellites with PRNs 1, 5, 7, 8

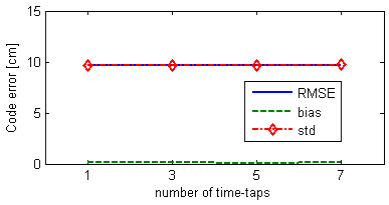

a) code error with MVDR STAP

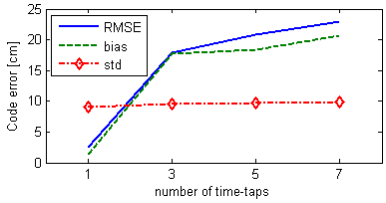

b) code error with MMSE STAP

Figure 7: Interference-free scenario. Results for code error on PRN 1

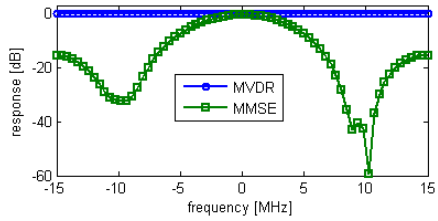

a) magnitude of STAP response

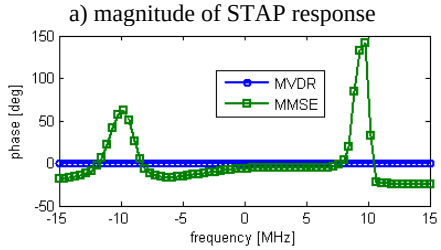

b) phase of STAP response

Figure 8: Interference-free scenario. 7-tap STAP response in direction of arrival of PRN 1

Continuous radio interference

In this simulation scenario four continuous radio interferers are added to the Galileo E5a signals and receiver noise of the previous scenario. Two of the interferers are assumed wideband with the double-sided bandwidth of 20 MHz and two other signals are continuous wave (i.e. sine-wave) interferers. All these four interferes have the same power level corresponding to the interference-to-noise ratio (INR) of 20dB and interference-to-signal ratio (ISR) of 51.9 dB. Other parameters of the continuous interferers can be found in Figure 5.

The time evolution of C/N_0 estimation obtained by the software receiver for PRN 1 after MVDR space-time processing is shown in Figure 9. The array processing started after 2000 ms of the receiver simulation resulted in the 6 dB increase of the estimated C/N_0 from 41.7 dB-Hz to 47.7 dB-Hz. This increase of C/N_0 with MVDR STAP option is independent of the number of taps (see Figure 6a). The dependency on the number of time taps appears only after 5000 ms when two wideband and two CW interferers are turned on. The increase of time taps from 1 to 7 has resulted in more than 11 dB improvement of C/N_0 in this scenario. A similar behaviour can be also observed for MMSE STAP in Figure 10a.

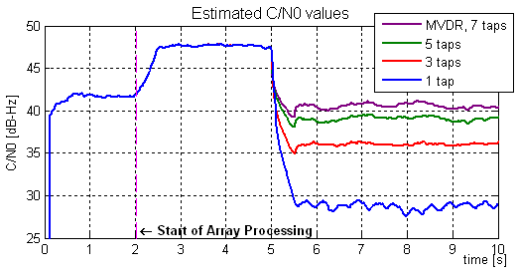

Figure 9: Continuous interference scenario. Estimated C/N_0 for PRN 1 after MVDR STAP

The results for the performance metrics presented in Figure 10 show the improvements achieved with the increase of the number of STAP time-taps. With 7 taps the test metrics achieve values which are the closest to the ones in the interference-free scenario (see Figure 6). With the MMSE option, the code tracking error with 7-tap STAP is even below the level of the interference free case. This is due to a flatter phase characteristic of the STAP frequency response in the continuous interference scenario (see Figure 8b and Figure 11b) and a correspondingly lower group delay caused by STAP. MVDR and MMSE algorithms show comparable performance in terms of code and Doppler tracking errors.

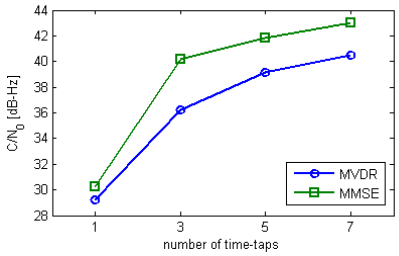

a) C/N_0

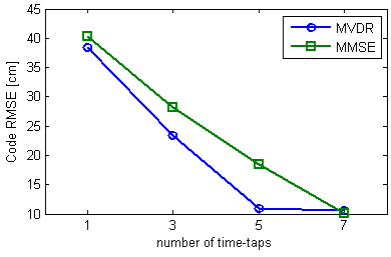

b) code error

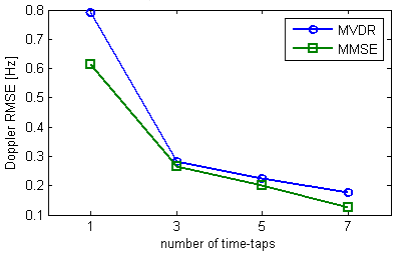

c) Doppler error

Figure 10: Continuous interference scenario. Performance metrics for PRN 1

The results for the STAP frequency response are shown in Figure 11. Uniform amplitude and phase characteristics of the STAP response are observed with the MVDR technique like in the interference-free scenario. In MMSE STAP case, the amplitude response shows a noticeable deviation from the one that has been observed in the interference-free case.

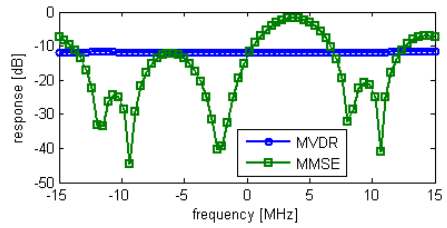

a) magnitude of STAP response

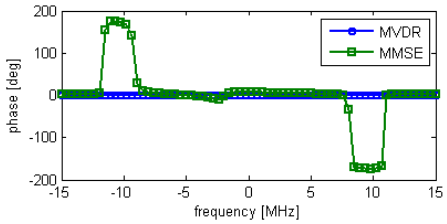

b) phase of STAP response

Figure 11: Continuous interference scenario. 7-tap STAP response in direction of arrival of PRN 1

The reception patterns of the antenna array with MVDR and MMSE STAP are presented in Figure 12. Spatial nulls in the directions of arrival of the continuous interferers (marked in the figure with red circles) can be observed with both STAP techniques. The direction to the Galileo E5a satellite is denoted in Figure 12 by a green circle.

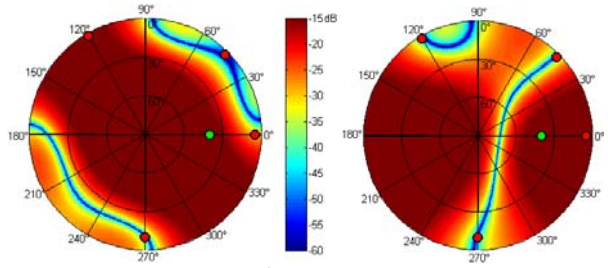

a) MVDR

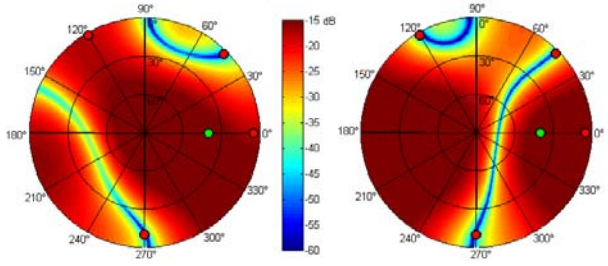

b) MMSE

Figure 12: Continuous interference scenario. Reception patterns for PRN 1 at f_{E5a} (left) and at $f_{RFI3} = f_{E5a}+5MHz$ (right)

Pulsed DME/TACAN radio interference

Three DME and two TACAN pulse trains were simulated using the signal parameters given in Figure 5b. The simulated DME and TACAN pulses are shown in Figure 13. A pulse blanker was optionally used in the software receiver for mitigating the DME/TACAN interference before STAP. The detection threshold in the pulse blanker was set to 3σ, where σ is the standard deviation of the receiver noise at the ADC input. The observed effective blanker duty circle with this threshold setting was about 9.7% which means that this percentage of the GNSS signals power was also lost after blanking out the DME/TACAN pulses. Without pulse blanking, the space-time adaptive processing was tested as a primary method for mitigating the pulsed interference, so that the overall performance with and without pulse blanking could be compared. The effect of the ADC bit resolution on the STAP performance without pulse blanking was also investigated by setting the ADC resolution to 4, 8 or 12 bits. The simulation results are presented in Figure 14 - Figure 16.

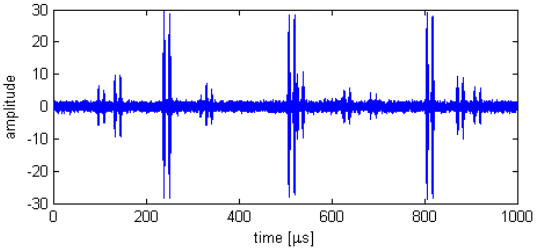

Figure 13: Pulsed DME/TACAN interference. Time plot of simulated pulse trains

The results for the performance metrics shown in Figure 14 and Figure 15 indicate that the combination of the pulse blanking with the space-time adaptive array processing performs better than the STAP alone. Even with a high ADC bit resolution and the maximum number of taps both MVDR and MMSE STAP options without pulse blanking cannot achieve the performance level with the blanking. The significant effect of the ADC bit resolution is observed only for the transition from 4-bit to 8-bit ADC. The further increase of the ADC bit resolution to 12 bit brings almost no performance improvement.

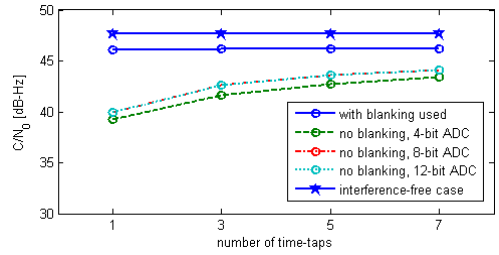

a) C/N_0

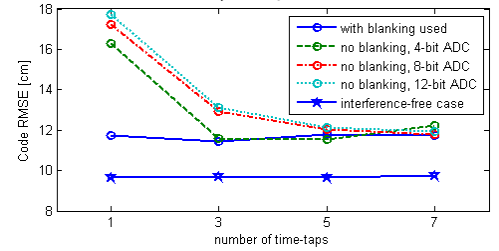

b) code error

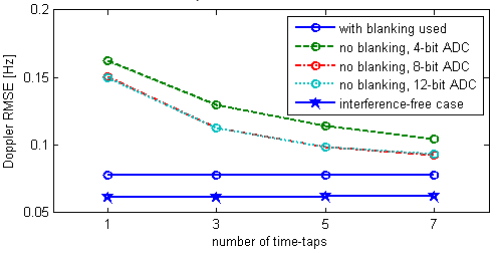

c) Doppler error

Figure 14: Pulsed DME/TACAN interference. Performance metrics with MVDR STAP for PRN 1

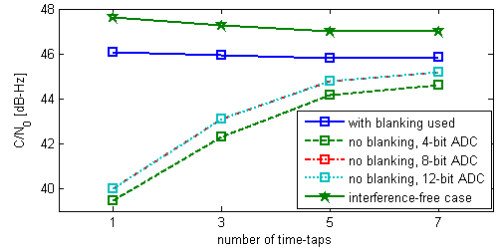

a) C/N_0

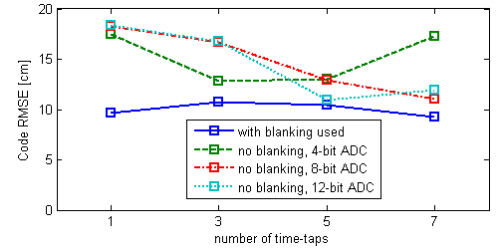

b) code error

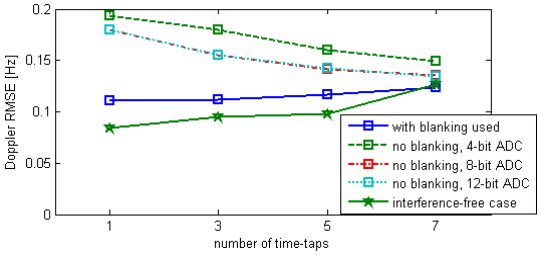

c) Doppler error

Figure 15: Pulsed DME/TACAN interference. Performance metrics with MMSE STAP for PRN 1

The effect of the pulse blanking on the amplitude and phase characteristics of the STAP frequency response can be clearly observed in Figure 16. With the pulse blanking being used, the amplitude response of the MMSE STAP option is close to the one of the interference-free case (see Figure 16a and Figure 8a). The MVDR STAP option shows flat amplitude and phase transfer characteristics both with the pulse blanking and without it.

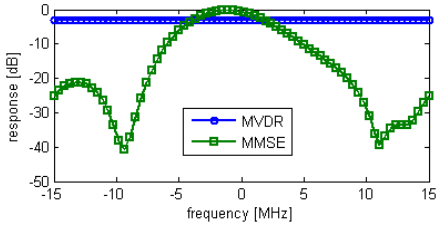

a) magnitude of STAP response, with pulse blanking

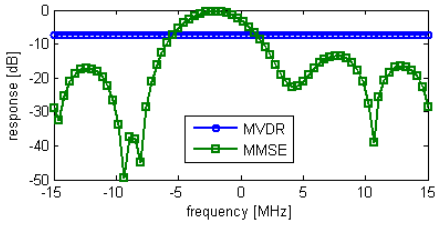

b) magnitude of STAP response, without pulse blanking, 8 bit ADC

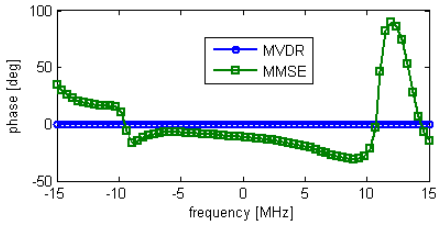

d) phase of STAP response, with pulse blanking

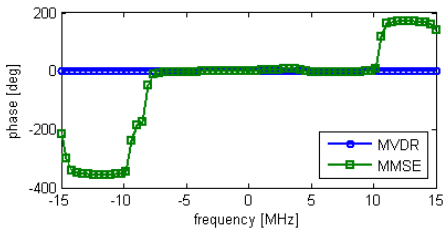

e) phase of STAP response, without pulse blanking, 8 bit ADC

Figure 16: Continuous interference scenario. 7-tap STAP response in direction of arrival of PRN 1

Scenario with continuous and pulsed DME/TACAN radio interferences

The combined scenario with both continuous and pulsed interference signals is a mixture of the two previous signal scenarios discussed above, which means that all interference signals indicated in Figure 5, b-c were simulated. The time plot of the output of an array element under these interference conditions is shown in Figure 17.

In the figure, no DME/TACAN pulse trains can be observed as these are masked by the strong continuous wideband and CW interferers. For visualisation purposes, the DME/TACAN pulse trains of the previous scenario are added in yellow to the graph for illustrating that point. It is obvious that the pulse blanking does not make any use in this interference situation.

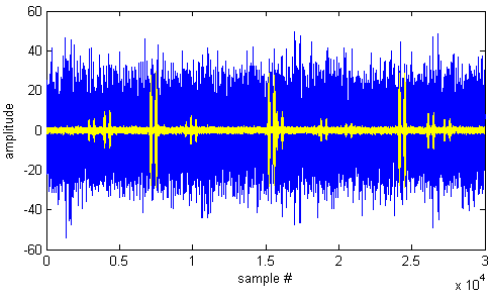

Figure 17: Combination of continuous and pulsed DME/TACAN interference. Time plot of an antenna output

The results for the carrier-to-noise density ratio estimated by the software receiver in the combined interference scenario are presented in Figure 18 where also the corresponding results from the interference-free scenario and the scenario with continuous interference are shown. The performance degradation with respect to the continuous interference scenario can be observed both with the MVDR and MMSE STAP options.

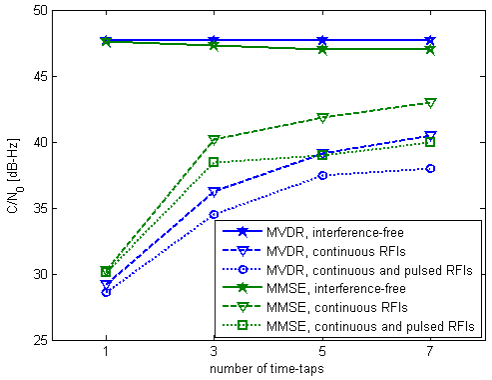

Figure 18: Combination of continuous and pulsed DME/TACAN interference. C/N_0 for PRN 1

The amplitude and phase of the STAP response are presented in Figure 19. As in previous scenarios, the MVDR STAP option allows for flat amplitude and phase transition characteristics and minimal distortions of the GNSS signal.

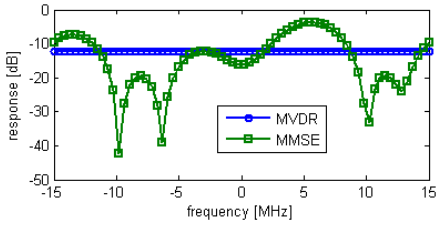

a) magnitude of STAP response

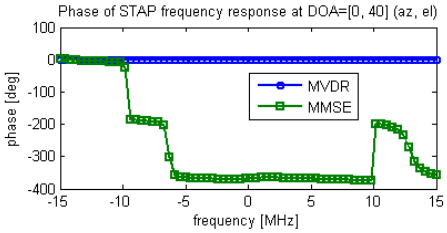

b) phase of STAP response

Figure 19: Combination of continuous and pulsed DME/TACAN interference. 7-tap STAP response in direction of arrival of PRN 1

SUMMARY AND CONCLUSIONS

In this paper we studied the mitigation of continuous and pulsed radio interferers with the help of space-time adaptive processing. The minimum variance distortionless response and the minimum mean square error techniques has been implemented in a multi-antenna MATLAB-based software receiver and their performance has been investigated by using the receiver simulations with tracking of Galileo E5a-Q signals. The test scenarios included continuous wideband and narrowband sine-wave interferers and the pulsed signals of DME/TACAN radio systems. In the pulsed interference scenario, the combination of the space-time adaptive processing and temporal pulse blanking has been tested.

The following conclusions can be drawn based on the obtained simulation results:

- The performance of tested STAP techniques improves with the number of time taps. The improvement becomes noticeable slower after 5 taps and therefore 5-7 taps may be considered as a trade-off between performance and complexity.
- In the pulsed DME/TACAN interference scenario the STAP techniques with the number of time taps of up to 7 showed performance level that is slightly below the one provided by a simple temporal pulse blanking. Therefore the combination of the space-time adaptive processing with the pulse blanking can be used in pulsed interference environments.
- In mixed scenarios, the pulsed interference may become masked by strong continuous interferers. In these conditions the performance of the pulse blanking depends on the detection threshold selection mechanism that was not in the scope of this study but could be investigated in the future.

- The results for STAP performance in the scenarios with DME/TACAN pulsed interference indicate that the effective mitigation of this type of interference can not be realised only with the temporal degrees of freedom.
- The tested STAP techniques provide comparable performance levels in the simulated interference scenarios. The constrained MVDR technique allows for keeping the STAP-induced phase and amplitude distortions of the useful GNSS signals at a very minimal level.

Future investigations may focus on the effects of antenna realistic characteristics including mutual coupling and calibration issues on the STAP performance.

REFERENCES

[1] R.L. Fante and J.J. Vaccaro, "Wideband Cancellation of Interference in a GPS Receive Array," IEEE Trans. on Aerospace and Electronic Systems, vol. 2, no. 2, , 2000, pp. 549-564.

[2] I.J. Gupta and T.D. Moore, "Space-Frequency Adaptive Processing (SFAP) for Interference Suppression in GPS Receivers," Proc. ION NTM, 2001, pp. 377-385.

[3] D.S. De Lorenzo, J. Rife, P. Enge, and D.M. Akos, "Navigation Accuracy and Interference Rejection for an Adaptive GPS Antenna Array," Proc. ION GNSS 2006, pp. 763-773.

[4] G. Carrie, F. Vincent, T. Deloues, D. Pietin, A. Renard, F. Letestu, "Optimal STAP Algorithms to GNSS Receivers", Proc. ENC-GNSS 2006, Manchester, UK.

[5] M. Kayton, R. F. Walter, "Avionics Navigation Systems", 2-nd Ed., 1997, John Wiley & Sons Inc., New York.

[6] Grace Xingxin Gao, "DME/TACAN Interference and its Mitigation in L5/E5 Bands", Proc. ION GNSS 2007, Fort Worth, Texas, September 2007.

[7] M. Cuntz, H. Denks, A. Konovaltsev, A. Hornbostel, A. Dreher, M. Meurer, "GALANT — Architecture Design and First Results of a Novel Galileo Navigation Receiver Demonstrator with Array Antennas", To be published in Proc. ION GNSS 2008, Savannah, GA.

[8] W. Au, L. Chen, K. Loo, A. Pabon, Y. Xiao, H.K. Hwang, "Simulation study of wideband interference rejection using STAP", Proc. IEEE Aerospace Conference, 2006.

[9] GSA: Galileo Open Service Signal-In-Space ICD, Draft 1, February 2008